Bipolar resistive switching behavior in Pt/Zn$_{1-x}$Mg$_x$O/pyrographite/Pt structure for memory application

Vikas Patel[1],* , Basumati Patel[2], Dhananjay Dhruv[3], Vishal Dhamecha[2], and Andrzej Nowicki[4]

[1] Sophisticated Instrumentation Centre for Applied Research and Testing (SICART), Vallabh Vidyanagar, Gujarat 388120, India
[2] Department of Electronics, Sardar Patel University, Vallabh Vidyanagar, Gujarat, India
[3] Natubhai V. Patel College of Pure and Applied Sciences, Vallabh Vidyanagar, Gujarat, India
[4] Institute of Nuclear Chemistry and Technology, Warsaw, Poland

ABSTRACT

Zn$_{1-x}$Mg$_x$O thin films have been deposited onhighly polished pyrographite substrates using pulsed laser deposition system in vacuum. Platinum electrodes were used to establish electrical contacts. Bipolar resistance behavior with a reproducible switching effect was observed in the Pt/Zn$_{1-x}$Mg$_x$O/pyrographite/Pt structure under DC sweeping voltage and pulsed mode operation. Only a low electric field is required to induce bistable switching states. The device properties of the bipolar switching device such as set/reset voltage resistance ratio were investigated. Based on the scanning electron micrographs and the corresponding current–voltage characteristics, it can be revealed that the switching phenomenon is dominated by the localization of the conducting filaments formed at the grain boundaries. The kinetics of the filament forming are found to be highly dependent on Zn$_{1-x}$Mg$_x$O microstructure. The fabricated device showed stable and reproducible bipolar resistive switching with reliable switching response for more than 10^3 cycles. The device exhibits good endurance and retention time under ambient conditions.

1 Introduction

The ongoing market demand for increased memory densities has forced the electronic industries for seeking new approaches to process and storage of information of nonvolatile memory technologies providing fast switching, high data density, and less power consumption [1, 2]. To improve the performance of nonvolatile memory device, understanding switching mechanism is a major challenge. A lot of materials such as transition metal oxides [3, 4], chalcogenide materials [5, 6], perovskites oxide [7–9] exhibit resistive switching effect and have attracted wide applications in the field of electronic industries.

Generally, two types of resistive switchings are found in previous literature: unipolar switching [10, 11] and bipolar switching [12, 13]. Numerous models have been proposed to understand the

Address correspondence to E-mail: vap@sicart.res.in

resistive switching mechanism such as conducting filaments [14, 15] the Mott transition in insulator [16, 17] and Schottky barrier model [18]. However, very few reports are available in the literature on the topic concerning changes in filaments morphology and composition after different switching cycles of resistive switching devices [19, 20]. Recent studies on resistive switching behavior of $Zn_{1-x}Mg_xO$-based devices have attracted many researchers for their wide application in semiconductor industries [21]. Usually, $Zn_{1-x}Mg_xO$ shows a hexagonal phase or cubic rock salt phase with an increase in *Mg* composition [22]. The growth and characterization of $Zn_{1-x}Mg_xO$ thin films and photo sensing performance with electro-optically efficient n-$Zn_{1-x}Mg_xO$/ p-Si heterojunction were reported by the authors previously [23, 24]. The resistive memory switching behavior in $ZnIn_2Se_4$ and $ZnGa_2Se_4$ thin films have been reported earlier [25, 26].

In the present investigation, scanning electron microscopy and current–voltage characteristic (I–V) were used to explain the formation and rupture of conducting filaments at the grain boundaries of platinum/$Zn_{1-x}Mg_xO$/pyrographite/platinum device. The device performance was confirmed with the help of retention and endurance test.

The striking finding of this research article was that the bipolar resistive switching effect was observed in the Pt/$Zn_{1-x}Mg_xO$/pyrographite/Pt stack with the reversible switching performances, when the applied bias amplitudes were regulated intentionally. The resistive switching characteristics were elucidated because of the controlled size of the conducting filament along with the pictorial SEM images obtained immediately after different switching cycles. Hence, this phenomenon provides new insight into the physical mechanism of the bipolar resistive switching device which is of great importance to the implementation of memory devices.

2 Experimental

The pulsed laser deposition (PLD) technique attached with KrF excimer laser (λ = 248 nm, 10 ns pulse duration) was used for deposition of $Zn_{1-x}Mg_xO$ (where x = 0.2) thin film at room temperature (303 K). The vacuum of the order of 5×10^{-4} Pa was maintained during $Zn_{1-x}Mg_xO$ thin film growth process. A highly polished pyrographite material

received from the Institute of Nuclear Chemistry and Technology (INCT), Warsaw, Poland was used as a substrate. The thin film $Zn_{1-x}Mg_xO$ was grown by allowing a suitable number of laser pulses on *ZnO* and *Mg* pellets (targets) to obtain uniform growth of thin films. The thickness of the deposited film was 1000 Å. The $Zn_{1-x}Mg_xO$ thin film shows n-type conductivity measured by Hall Effect experiment [24]. The electrical characterization (I–V) of Pt/ $Zn_{1-x}Mg_xO$/pyrographite/Pt structure was carried out with a set-up consisting of two platinum wires with circular end (diameter of $\approx$ 200 μm) connected with a weak cantilever as shown in Fig. 1a. By applying proper pressure to the platinum wires, the electrical contacts were established on the top surface of $Zn_{1-x}Mg_xO$ film and on pyrographite surface.

Figure 1b shows the X-ray diffractogram of Pt/ $Zn_{1-x}Mg_xO$/pyrographite/Pt structure. The d-spacing values obtained from Pt/$Zn_{1-x}Mg_xO$/pyrographite/Pt structure thin films from (002), (101), (110), (112), and (202) planes nicely match with the
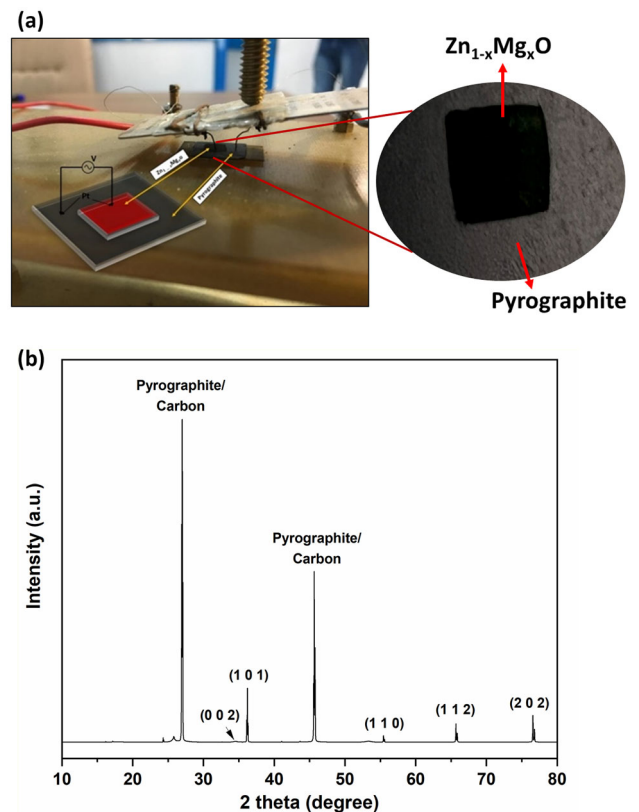

Fig. 1 **a** Schematic of the Pt/$Zn_{1-x}Mg_xO$/pyrographite/Pt cell for electric characterization. **b** X-ray diffractogram of Pt/$Zn_{1-x}Mg_xO$/ pyrographite/Pt structure

standard data obtained from International Centre for Diffraction Data (File No. ICDD 01-078-3032).

The energy-dispersive analysis of X-rays (EDAX) (Model: FEG-SEM 450 Nano Nova SEM, Make: FEI, Netherland) was used for atomic composition and surface morphological study of $Zn_{1-x}Mg_xO$ thin films. A semiconductor characterization system (Model: Keithely 4200, USA) and a source meter (Model: Keithely 602 A, USA) which is equipped with a personal computer (having TSP express software) in a pulse generator mode were employed for electrical characterization (I–V) of pristine device at 303 K.

3 Results and discussion

Figure 2a and b shows the surface plan view of SEM micrographs of $Zn_{1-x}Mg_xO$ thin film deposited onpyrographite substrate at ambient temperature and annealed at 573 K for 1 h under vacuum, respectively.

The film deposited at room temperature has random orientation of crystallites with the average grain size of ≈ 2.5 μm. After annealing the film had improved crystallinity with average grain size ≈ 5.4 μm. The cross-sectional SEM micrograph of $Pt/Zn_{1-x}Mg_xO/Pyrographite/Pt$ memory device is depicted in Fig. 2c which shows average thickness of $Zn_{1-x}Mg_xO$/pyrographite interface as 5.646 μm. Figure 3 illustrates the typical current–voltage (I–V) characteristics of $Pt/Zn_{1-x}Mg_xO$/pyrographite/Pt device by applying voltage in sweep and pulse mode in order to study resistive switching effect.

Generally, electroforming process is required just prior to the device undergoes into a switching state. In order to initiate the forming process, 5–6 cycles were applied to activate the pristine device. After forming the device, the sweep voltages were applied to the top Pt electrode (TE), i.e., on the surface of $Zn_{1-x}Mg_xO$ thin film in the sequence of $(0 \rightarrow +0.5 V \rightarrow 0 \rightarrow -0.5 V \rightarrow 0)$, while the bottom Pt electrode (BE) placed on the surface of pyrographite was grounded. When the applied voltage starts sweeping from 0 to 0.12 V, the current slightly increases. Further, increase in bias from 0.12 to 0.3 V the current gradually increases (0.5×10^{-4} A) up to the current compliance limit of 1 mA as shown in

Fig. 3. This change in current will switch the device from high resistance state (HRS) to low resistance state (LRS). This behavior is known as SET process whereby the compliance current limit is kept at 1 mA in order to prevent permanent damage of the device and maintained up to 0.5 V to 0.25 V. The device remained in SET position during the applied reverse sweep from 0.5 V. After further decreasing the applied bias from 0.25 to 0 V, the current decreases linearly and maintains its linear behavior. The same linear behavior is observed in opposite polarity down to a reverse bias (TE negative voltage) of -0.3 V with a -6×10^{-4}A current. The linear relationship between current and voltage existing between $+0.25$ V and -0.3 V signifies that the device is switching back from LRS to HRS. The current decreases slightly, indicating the 'reset' process during -0.3 V to -0.5 V reverse voltage. When voltage sweeps from -0.5 V to 0 V, the current drops suddenly and the device returns to HRS. The two states, SET and RESET, remain almost unchanged by changing the voltage polarity at top Pt electrode [27] as shown in Fig. 3. The device switches between LRS/HRS with a resistance ratio ≈ 10 at 0.3 V.

The study of memory device in pulse mode is essential for the enhanced understanding of the conduction mechanism and in-turn it reduces the heating effect due to time delay during which the conductance of the device switch back to the previous state [28] as depicted in Fig. 4.

A pulse of $+0.5$ V and 1 μs duration switching the system into the low resistance state and data is written in the memory device. After applying a negative pulse of -0.5 V of 1 μs duration, the data written to the device is erased and device returns to high resistance state. Between each sequence of LRS/HRS operations, the current in the device was consecutively read at 0.1 V for eight times. The repeated switching behavior over a period of 200 s indicates that the device possesses good endurance which is a very important property of any memory device.

To acquire the further insight in to the switching phenomenology of the pristine memory device, a generalized filament model is presented. The bipolar resistive switching mechanism may be explained by ionic migration which is due to Joule heating effect and applied electric field [29, 30]. It is well known that the defects such as oxygen vacancies and
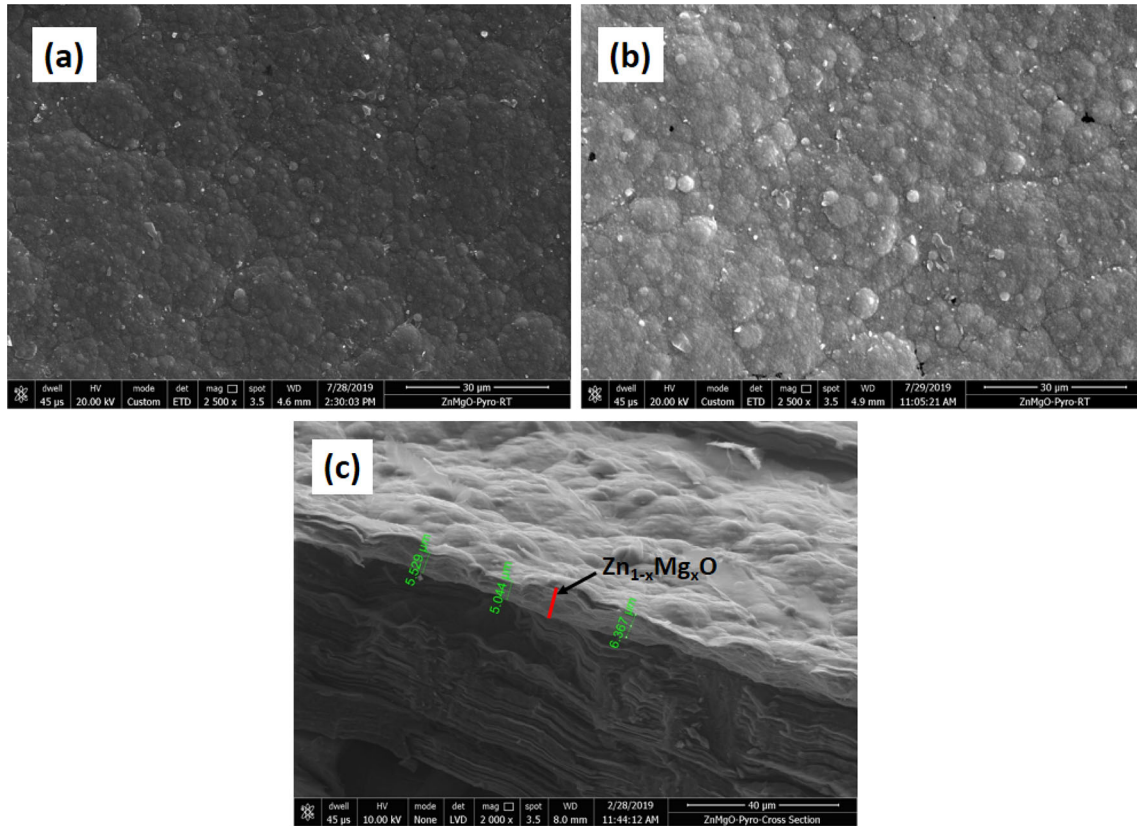
Fig. 2 SEM image of $Zn_{1-x}Mg_xO$ thin film deposited on pyrographite substrates (**a**) as deposited (303 K). SEM images of $Zn_{1-x}Mg_xO$ thin film deposited on pyrographite substrates (**b**) annealed at 573 K for 1 h. Cross-sectional SEM images of $Zn_{1-x}Mg_xO$ thin film deposited on pyrographite substrates (**c**)
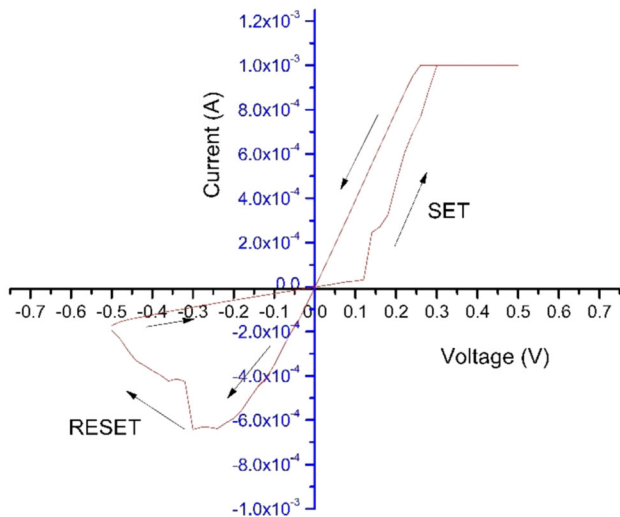

Fig. 3 Current–voltage (IV) Characteristic of formed Pt/$Zn_{1-x}Mg_xO$/Pyrographite/Pt device

interstitial atoms exist in polycrystalline oxide thin film. The $Zn_{1-x}Mg_xO$ thin film shows n-type conductivity with a wide band gap (E_g = 3.7 eV) semiconductor [31]. It is well known that the Pt electrode (TE) has high oxygen mobility in it [32]. Therefore, release of oxygen ions from Pt electrode to Pt/$Zn_{1-x}Mg_xO$ thin film interface or vice versa must be fast and active after the application of bias voltage.

In normal condition, during first cycle of (0 V → + 0.5 V → 0 V), SET (LRS) occurs in pristine device. It is assumed that the oxygen ions are attracted from the oxide to the reactive electrode (TE) when + V was applied to the TE as shown in Fig. 5a (Left Hand Side). The immediate SEM image (right hand side) after the switching operation shows the presence of local formation of conducting filament at grain boundaries of the oxide films. The EDAX analysis of the filament confirm that it is *Zn* rich and

Fig. 4 A sequence of input voltage pulses applied to the pristine device and corresponding output current at each voltage pulse
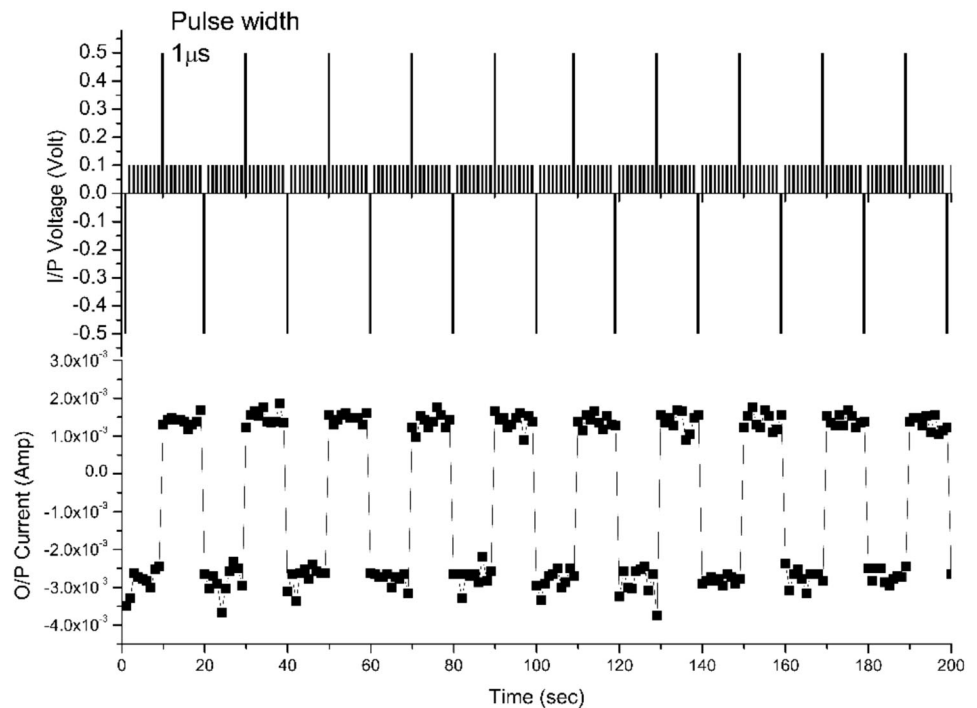
oxygen deficient. As it is evident from Fig. 5a (Right Hand Side) that when the voltage was applied during SET process, Zn diffusion takes place along the grain boundaries contributing for the local filament formation providing driving force for the switching mechanism. Inversely, applying $- V$ to the reactive electrode (TE) $(0\ V \rightarrow - 0.5\ V \rightarrow 0\ V)$, repels the oxygen from the reactive electrode to the oxide, so that filament is raptured (switching from LRS to HRS) near the electrode/oxide interface due to local Joule heating [32] as shown in Fig. 5a (right hand side). The conductive filament is not actively dissolved after the reset process, rather only disconnected near the grain boundaries.

During the five cycle $(0\ V \rightarrow\ + 0.5\ V \rightarrow 0\ V \rightarrow - 0.5\ V \rightarrow 0\ V)$, Fig. 5(b) (left hand side), the switching effect starts at relatively lower voltage of 0.1 V with increase in current. As it is evident from the Fig. 5b right hand side that tiny metallic filaments gather-together near the pre-existing filament to form stronger and more conducting filaments in LRS state.

Repeating the sweep measurements after ten cycles confirmed reproducible bipolar resistive switching voltages with same SET/RESET values as shown in Fig. 5c (left hand side). The pictorial SEM image

Fig. 5c (Right hand side) shows that the extension of the branch filaments generated along the grain boundaries near the existing filaments, stabilizing the multifilament channel involving the SET process.

The multi filament disassembles, while weak filament remains during switch back to RESET. The study of the data retention provides insight into the switching mechanism observed under SET/RESET operations at room temperature (300 K) as shown in Fig. 6. In each DC sweep, the resistance values are read at 0.1 V. The LRS remains almost stable and HRS shows slight fluctuation in the beginning stage of operation up to 100 s. Obviously, the resistance of LRS and HRS exhibited no degradation up to 1 week, indicating good retention characteristics of both states.

4 Conclusion

The bipolar resistive switching characteristics were observed in Pt/$Zn_{1-x}Mg_xO$/Pyrographite/Pt memory device by electrically induced resistance switching between LRS and HRS with a resistance ratio HRS/LRS of 10. The conduction mechanism of LRS to
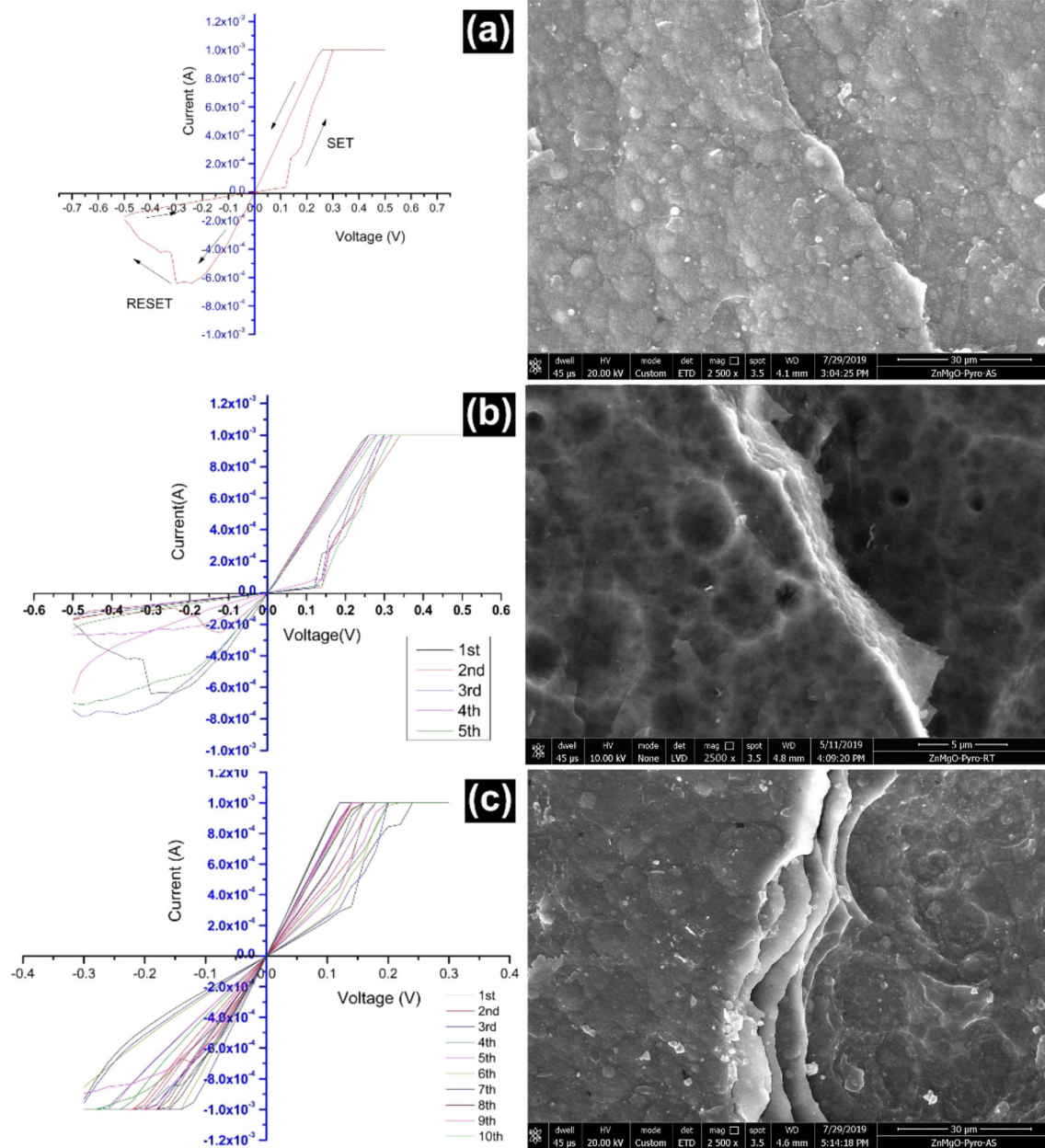
Fig. 5 a–c The electrical behavior and the corresponding surface morphology taken immediately after the switching of the device

HRS are consistent with the filament theory. The filament model with SEM pictorial evidence supports the switching phenomenon which is associated with the formation and rapture of the conducting filaments consisting of oxygen vacancies/metallic ions migration at the grain boundaries of the oxide films.

The device exhibited good retention, a low power consumption and better SET/ RESET voltage distribution, suggesting that $Pt/Zn_{1-x}Mg_xO/Pyro$-graphite/Pt memory device has great potential for future memory applications.
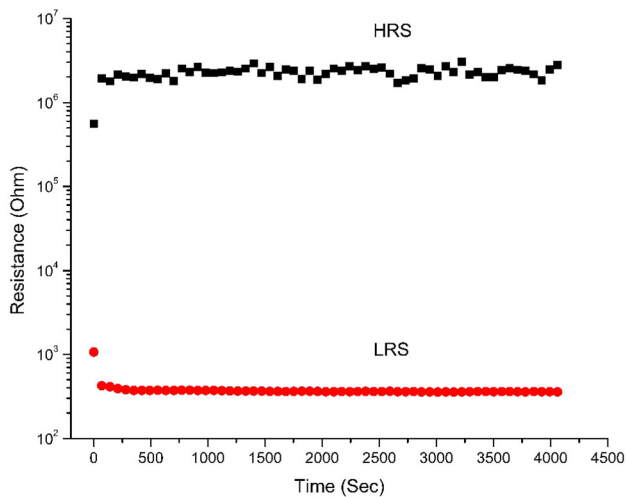
Fig. 6 Resistance evolution of the Pt/Zn$_{1-x}$Mg$_x$O/Pyrographite/Pt device

Author contributions

VP contributed to the investigation, conceptualization, writing the original draft, formal analysis, and methodology. BHP contributed to the conceptualization, investigation, editing, supervision, methodology, and writing the original draft. DD contributed to data curation and formal analysis. VD contributed to data curation. AN contributed to data curation.

Data availability

The data that support the findings of this study are available within the article.

Declarations

Conflict of interest The authors declare that they have no known competing financial interests or personal relationships that could have appeared to influence the work reported in this paper. The authors declare the following financial interests/ personal relationships which may be considered as potential competing interests:

References

1. R. Waser, R. Dittmann, C. Staikov, K. Szot, Redox-based resistive switching memories nanoionic mechanisms, prospects, and challenges. Adv. Mater. **21**(25–26), 2632–2663 (2009). https://doi.org/10.1002/adma.200900375

2. V. Gupta, S. Kapur, S. Saurabh, A. Grover, Resistive random access memory: a review of device challenges. IETE Tech. Rev. (Institution Electron. Telecommun. Eng. India) **37**(4), 377–390 (2020). https://doi.org/10.1080/02564602.2019.1629341

3. Q. Liu, W. Guan, S. Long, R. Jia, M. Liu, J. Chen, Resistive switching memory effect of Zr O$_2$ films with Zr+ implanted. Appl. Phys. Lett. **92**(1), 90–93 (2008). https://doi.org/10.1063/1.2832660

4. T.H. Hou, K.L. Lin, J. Shieh, J.H. Lin, C.T. Chou, Y.J. Lee, Evolution of RESET current and filament morphology in low-power HfO$_2$ unipolar resistive switching memory. Appl. Phys. Lett. **98**(10), 2–5 (2011). https://doi.org/10.1063/1.3565239

5. S.Q. Liu, N.J. Wu, A. Ignatiev, Electric-pulse-induced reversible resistance change effect in magnetoresistive films. Appl. Phys. Lett. **76**(19), 2749–2751 (2000). https://doi.org/10.1063/1.126464

6. S.C. Oh, H.Y. Jung, H. Lee, Effect of the top electrode materials on the resistive switching characteristics of TiO$_2$ thin film. J. Appl. Phys. **109**(12), 633–636 (2011). https://doi.org/10.1063/1.3596576

7. R. Waser, M. Aono, Nanoionics-based resistive switching memories. Nanosci. Technol. A Collect. Rev. Nat. J. **6**(11), 833–840 (2007). https://doi.org/10.1142/9789814287005_0016

8. A. Pradel, N. Frolet, M. Ramonda, A. Piarristeguy, M. Ribes, Bipolar resistance switching in chalcogenide materials. Phys. Status Solidi Appl. Mater. Sci. **208**(10), 2303–2308 (2011). https://doi.org/10.1002/pssa.201000767

9. B. Dey et al., Electrical switching behaviour of a metalloporphyrin in Langmuir-Blodgett film. Org. Electron. **55**, 50–62 (2018). https://doi.org/10.1016/j.orgel.2017.12.038

10. W.Y. Chang, Y.C. Lai, T.B. Wu, S.F. Wang, F. Chen, M.J. Tsai, Unipolar resistive switching characteristics of ZnO thin films for nonvolatile memory applications. Appl. Phys. Lett. **92**(2), 1–4 (2008). https://doi.org/10.1063/1.2834852

11. X. Chen, G. Wu, D. Bao, Resistive switching behavior of Pt/Mg$_{0.2}$Zn$_{0.8}$O/Pt devices for nonvolatile memory applications. Appl. Phys. Lett. (2008). https://doi.org/10.1063/1.2978158

12. A.A. Patil et al., Bipolar-resistive switching and memristive properties of solution-processable cobalt oxide nanoparticles. J. Mater. Sci. Mater. Electron. **31**(12), 9695–9704 (2020). https://doi.org/10.1007/s10854-020-03515-3

13. C.C. Lin, B.C. Tu, C.C. Lin, C.H. Lin, T.Y. Tseng, Resistive switching mechanisms of V-doped SrZrO$_3$ memory films. IEEE Electron Device Lett. **27**(9), 725–727 (2006). https://doi.org/10.1109/LED.2006.880660

14. F. Zahoor, T. Zainal Azni Zulkifli, F. Ahmad Khanday, NANO REVIEW open access resistive random access memory (RRAM): an overview of materials, switching mechanism, performance, multilevel cell (mlc) storage, modeling, and applications. Nanoscale Res. (2020). https://doi.org/10.1186/s11671-020-03299-9

15. B.J. Choi et al., Resistive switching mechanism of TiO$_2$ thin films grown by atomic-layer deposition. J. Appl. Phys. (2005). https://doi.org/10.1063/1.2001146

16. M. Fujimoto et al., TiO$_2$ anatase nanolayer on TiN thin film exhibiting high-speed bipolar resistive switching. Appl. Phys. Lett. (2006). https://doi.org/10.1063/1.2397006

17. M.J. Rozenberg, I.H. Inoue, M.J. Sánchez, Nonvolatile memory with multilevel switching: a basic model. Phys. Rev. Lett. **92**(17), 1–4 (2004). https://doi.org/10.1103/PhysRevLett.92.178302

18. A. Sawa, T. Fujii, M. Kawasaki, Y. Tokura, Hysteretic current-voltage characteristics and resistance switching at a rectifying Ti/Pr$_{0.7}$Ca$_{0.3}$MnO$_3$ interface. Appl. Phys. Lett. **85**(18), 4073–4075 (2004). https://doi.org/10.1063/1.1812580

19. A. Beck, J.G. Bednorz, C. Gerber, C. Rossel, D. Widmer, Reproducible switching effect in thin oxide films for memory applications. Appl. Phys. Lett. **77**(1), 139–141 (2000). https://doi.org/10.1063/1.126902

20. J.W. Lee, W.J. Cho, Fabrication of resistive switching memory based on solution processed PMMA-HfOx blended thin films. Semicond. Sci. Technol. (2017). https://doi.org/10.1088/1361-6641/aa5133

21. X. Chen, G. Wu, P. Jiang, W. Liu, D. Bao, Colossal resistance switching effect in Pt/spinel-MgZnO/Pt devices for nonvolatile memory applications. Appl. Phys. Lett. **94**(3), 2012–2015 (2009). https://doi.org/10.1063/1.3073858

22. Z. Vashaei et al., Structural variation of cubic and hexagonal Mg$_x$Zn$_{1-x}$O layers grown on MgO(111)/c—sapphire. J. Appl. Phys. (2005). https://doi.org/10.1063/1.2039273

23. V. Patel, B. Patel, V. Dhamecha, D. Dhruv, Fabrication of ZnMgO thin films by pulsed laser deposition method. Indian J. Tech. Educ., pp. 176–178 (2017)

24. V. Patel, B.H. Patel, Photo sensing performance with electro-optically efficient n-Zn$_{1-x}$Mg$_x$O/p-Si heterojunction. J. Mater. Sci. Mater. Electron. (2021). https://doi.org/10.1007/s10854-021-06110-2

25. D.K. Dhruv, A. Nowicki, B.H. Patel, V.D. Dhamecha, Memory switching characteristics in amorphous ZnIn$_2$Se$_4$ thin films. Surf. Eng. **31**(7), 556–562 (2015). https://doi.org/10.1179/1743294415Y.0000000001

26. V. Dhamecha, B. Patel, D. Dhruv, A. Nowicki, Resistive switching memory effects in chalcogenide semiconductor ZnGa$_2$Se$_4$ thin films. Surf. Eng. **36**(1), 100–105 (2020). https://doi.org/10.1080/02670844.2019.1625505

27. A. Tschöpe, Interface defect chemistry and effective conductivity in polycrystalline cerium oxide. J. Electroceram. **14**(1), 5–23 (2005). https://doi.org/10.1007/s10832-005-6580-6

28. T. Li, H. Yu, S.H.Y. Chen, Y. Zhou, S.T. Han, The strategies of filament control for improving the resistive switching performance. J. Mater. Chem. C **8**(46), 16295–16317 (2020). https://doi.org/10.1039/d0tc03639k

29. J.R. Bosnell, C.B. Thomas, Preswitching electrical properties, 'forming', and switching in amorphous chalcogenide alloy threshold and memory devices. Solid State Electron. (1972). https://doi.org/10.1016/0038-1101(72)90047-0

30. Y. Zhang et al., Structural and photoluminescence properties of Zn$_{0.8}$Mg$_{0.2}$O thin films grown on Si substrate by pulsed laser deposition. Thin Solid Films **458**(1–2), 161–164 (2004). https://doi.org/10.1016/j.tsf.2003.12.127

31. F. Nardi, S. Larentis, S. Balatti, D.C. Gilmer, D. Ielmini, Resistive switching by voltage-driven ion migration in bipolar RRAMPart I: experimental study. IEEE Trans. Electron Devices **59**(9), 2461–2467 (2012). https://doi.org/10.1109/TED.2012.2202319

32. A. Grill, W. Kane, J. Viggiano, M. Brady, R. Laibowitz, Base electrodes for high dielectric constant oxide materials in silicon technology. J. Mater. Res. **7**(12), 3260–3265 (1992). https://doi.org/10.1557/JMR.1992.3260